TELKOMNIKA Telecommunication Computing Electronics and Control
Vol. 20, No. 4, August 2022, pp. 731~739
ISSN: 1693-6930, DOI: 10.12928/TELKOMNIKA.v20i4.23769

Throughput analysis of power beacon-aided multi-hop MIMO relaying networks employing NOMA and TAS/SC

Pham Minh Nam[1], Thanh-Long Nguyen[2], Ha Duy Hung[3], Tran Trung Duy[4], Nguyen Thanh Binh[4], Nguyen Luong Nhat[4]
[1]Faculty of Electronics Technology, Industrial University of Ho Chi Minh City, Ho Chi Minh City, Vietnam
[2]Faculty of Information Technology, Ho Chi Minh City University of Food Industry, Ho Chi Minh City, Vietnam
[3]Wireless Communications Research Group, Faculty of Electrical and Electronics Engineering, Ton Duc Thang University, Ho Chi Minh City, Vietnam
[4] Faculty of Electrical Engineering, Posts and Telecommunications Institute of Technology, Ho Chi Minh City, Vietnam

Article Info

Article history:

Received Sep 26, 2021
Revised Apr 21, 2022
Accepted May 05, 2022

Keywords:

Multi-hop relaying networks
NOMA
TAS/SC
Throughput
Wirelessly energy harvesting

ABSTRACT

This paper measures end-to-end (e2e) throughput of power beacon-assisted multi-hop decode-and-forward (DF) relaying scheme adopting non-orthogonal multiple access (NOMA) and transmit antenna selection (TAS)/selection combining (SC). Particularly, TAS/SC and NOMA are adopted at each hop to relay different data of a source to multiple destinations. Moreover, the transmitters including source and relays have to harvest wireless energy from radio frequency (RF) signals from a power beacon. We also propose a simple and efficient power allocation method for the signals transmitted at each hop. For performance measurement and comparison, we provide closed-form formulas of the e2e throughput over Rayleigh fading channel. We then verify our derivations by computer simulations as well as compare the e2e throughput performance between our scheme and the corresponding one that does not use NOMA.

Corresponding Author:

Thanh-Long Nguyen
Faculty of Information Technology, Ho Chi Minh City University of Food Industry
Ho Chi Minh City, 70000, Vietnam.
Email: longnt@hufi.edu.vn

1. INTRODUCTION

Multi-hop relaying (MHR) [1]-[6] is commonly adopted to improve the end-to-end (e2e) performance for wireless networks when a source cannot directly send its data to a far destination. Therefore, MHR often employs intermediate nodes (called relays) to help the source-destination communication. In [1], [2], [5] the relays employed amplify-and-forward (AF) mode to forward the received data to their next node. In [3]-[6], the relays performed decode-and-forward (DF) mode, where they decoded, re-encoded, and then sent the received data to the next hop. The DF relaying often outperforms the corresponding AF one due to the noise removal.

The main disadvantages of MHR are high e2e delay time and low throughput since the transmission is realized via multiple orthogonal time slots [1]-[6]. Indeed, if the number of hop is K, the maximum e2e throughput is $1/K$, i.e., one data per K time slots. Although published works [4], [6]-[8] proposed various diversity-based MHR approaches (i.e., path selection [4], relay selection [6], transmit antenna selection (TAS)/selection combining (SC) [7], [8]) for performance enhancement, the obtained e2e throughput is still $1/K$.

Non-orthogonal multiple access (NOMA) [9]-[12] can be used to obtain higher e2e throughput for MHR. In NOMA, the source can simultaneously send different data to the destinations which can adopt successive interference cancellation (SIC) to extract the desired data. In [13], NOMA is applied in MHR under presence of an active eavesdropper. Since the source can send two data to the destination at the same time, the e2e throughput obtained in [13] is $2/K$. Moreover, the transmitters in [13] must adjust their transmit power, follows the instantaneous channel state information (CSI) of the eavesdropping links.

Recently, radio frequency (RF) energy harvesting (RF-EH) [14], [15] has been reported in a lot of literature. One of efficient RF-EH models is to deploy power beacon stations [16]-[18] for charging the wireless devices within a certain area. Xu *et al.* [19], [20] studied the RF-EH based MHR employing the RF power beacon stations in underlay cognitive radio networks. Tin *et al.* [21] proposed the power beacon-aided MHR scheme, where NOMA is employed to send multiple data from the source to the destination. Vo *et al.* [22] studied the RF-EH NOMA MHR to optimize e2e secrecy performance.

This paper proposes the RF-EH based DF MHR using power beacon and NOMA. In the proposed scheme, the source, relay and destination nodes are multi-antenna wireless devices, and TAS/SC is adopted at each hop to relay the source data. Next, the main difference between our proposed scheme and the existing ones related to MHR is presented as:
- Different with [13], our scheme considers the RF-EH MHR method, and the transmitters and receivers in this paper are equipped with multiple antennas. Moreover, published work [13] studied physical-layer security with presence of the active eavesdropper.
- Unlike [19], [20], the NOMA-based transmission is used to improve the e2e throughput, while the authors of [19], [20] considered the underlay cognitive environment.
- The main difference between this paper and our previous work [21] can be listed as: i) this paper studies the multi-input multi-output (MIMO) scenario that employs TAS/SC; ii) the source in this paper attempts to send its data to multiple destinations while only one destination is considered in [21]; and iii) this paper does not consider the hardware impairments as in [21].
- The main difference between this paper and the related work [22] can be summarized as: i) this paper concerns with the e2e throughput performance; ii) the transmitter and receiver nodes in this paper are equipped with multiple antennas, and TAS/SC is adopted at each hop; and iii) this paper does not consider the physical-layer security as in [22].

Next, we will summarize the main contribution of this paper as:
- We propose the wirelessly EH MHR scheme, where the TAS/SC and NOMA techniques are employed to obtain better performance, in terms of the e2e throughput and reliability of the data transmission.
- We propose a simple and efficient power allocation method for the signals transmitted at each hop.
- We derive closed-form expressions of the total e2e throughput for the proposed scheme over Rayleigh fading channel. We then verify our derivations via Monte Carlo simulations, i.e., the presented results show that the simulation and theoretical results are in an excellent agreement.
- The proposed scheme can obtain better performance as compared with the corresponding MHR that does not use NOMA.

The rest of this paper is organized as follows. The system model of the proposed RF-EH MHR with TAS/SC and NOMA is presented in section 2. Section 3 derives exact expressions of the e2e throughput. The simulation and theoretical results are given in section 4. Finally, section 5 concludes this paper.

2. SYSTEM MODEL

In Figure 1, the source T_0 applies the NOMA technique to send N data to N destinations denoted $T_{K,n}$, where $n \in [1, N]$. The transmitter T_k harvests RF energy from the single-antenna power beacon (B) for transmitting the data, where $k \in [0, K-1]$, where B uses different frequencies with T_k. Without loss of generality, assume that the T_k and $T_{K,n}$ nodes have L receive and transmit antennas. In addition, the source-destination transmission is split into K orthogonal time slots, and TAS/SC is performed at each hop.

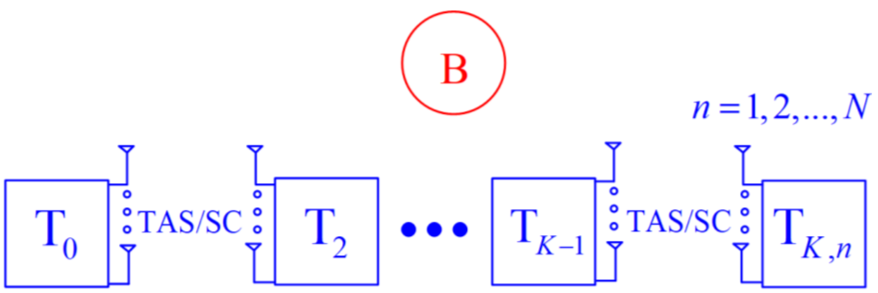

Figure 1. System model of the proposed RF-EH MHR scheme with TAS/SC and NOMA

Let us denote $\gamma_{X^{(a)}Y^{(b)}}$ as the channel gain between the a-th antenna of the node X and the $b\text{-}th$ antenna of the node Y. Note that in case that X or Y has only a single antenna, the indices a and b are skipped. When the channel is Rayleigh fading, $\gamma_{X^{(a)}Y^{(b)}}$ is an exponential random variable, and cumulative distribution function (CDF) and probability density function (PDF) of $\gamma_{X^{(a)}Y^{(b)}}$ are:

$$F_{\gamma_{X^{(a)}Y^{(b)}}}(z) = 1 - exp(-\lambda_{\mathrm{XY}} z)\,, f_{\gamma_{X^{(a)}Y^{(b)}}}(z) = \lambda_{\mathrm{XY}}\, exp(-\lambda_{\mathrm{XY}} z) \quad (1)$$

Where:
$\lambda_{\mathrm{XY}} = (d_{\mathrm{XY}})^{\beta}$ [21], β is a path-loss exponent, and d_{XY} is the $X\text{–}Y$ distance.

If the e2e delay time is 1 (time unit), the time allocated for each time slot is $\tau = 1/K$. Moreover, at each time slot, the time of $\alpha\tau$ is spent for the EH phase, and the remaining time of $(1-\alpha)\tau$ is spent for the data transmission. Considering the $k\text{-}th$ time slot; the energy harvested by T_{k-1} is given as:

$$E_{T_{k-1}} = \eta\alpha\tau P_B \sum_{m=1}^{L} \gamma_{\mathrm{BT}_{k-1}^{(m)}} = \eta\alpha\tau P_B X_{k-1}^{\mathrm{sum}} \quad (2)$$

Where:
P_B is transmit power of B, η is energy conversion efficiency $(0 \le \eta \le 1)$, and $X_{k-1}^{\mathrm{sum}} = \sum_{m=1}^{L} \gamma_{\mathrm{BT}_{k-1}^{(m)}}$.
Then, the average transmit power of T_{k-1} in the data transmission phase can be expressed as:

$$P_{T_{k-1}} = \frac{E_{T_{k-1}}}{(1-\alpha)\tau} = \mu P_B X_{k-1}^{\mathrm{sum}} \quad (3)$$

Where:
$\mu = \frac{\eta\alpha}{(1-\alpha)}$. After the EH phase, T_{k-1} linearly combines N signals to obtain a superimposed signal.

$$x_k^{\oplus} = \sum_{n=1}^{N} \sqrt{a_n P_{T_{k-1}}}\, x_n \quad (4)$$

Where:
x_n is the signal of $T_{K,n}$, a_n are coefficients: $\sum_{n=1}^{N} a_n = 1$ and $1 > a_1 > a_2 > \ldots > a_N > 0$.
Before sending $x_k^{\oplus}$, the nodes T_{k-1} and T_k cooperate to perform the TAS/SC technique as in [7].

$$\gamma_{T_{k-1}^{(t_{k-1})} T_k^{(r_k)}} = \max_{a=1,\ldots,L}\left(\max_{b=1,\ldots,L}\left(\gamma_{T_{k-1}^{(a)} T_k^{(b)}}\right)\right) \quad (5)$$

Where:
t_{k-1} and r_k are the selected transmit and receive antennas at T_{k-1} and T_k, respectively.

After receiving $x_k^{\oplus}$ from T_{k-1}, T_k performs SIC to decode all the signals. Similar to [21], from (3), the instantaneous signal-to-noise ratio (SNR) obtained for decoding x_n can be written as:

$$\psi_{k,x_n} = \frac{a_n \mu \Delta X_{k-1}^{\mathrm{sum}} \gamma_{T_{k-1}^{(t_{k-1})} T_k^{(r_k)}}}{\left(\sum_{i=n+1}^{N} a_i\right)\mu\Delta X_{k-1}^{\mathrm{sum}} \gamma_{T_{k-1}^{(t_{k-1})} T_k^{(r_k)}} + 1}\,(n < N); \text{and} \psi_{k,x_N} = a_N \mu \Delta X_{k-1}^{\mathrm{sum}} \gamma_{T_{k-1}^{(t_{k-1})} T_k^{(r_k)}} \quad (6)$$

Where:
$\Delta = P_B/\sigma^2$, with σ^2 is variance of Gaussian noises at T_k (also at all of the receivers).
Then, the instantaneous channel capacity of x_n at the k-th time slot is calculated as:

$$C_{k,x_n} = (1-\alpha)\tau\, log_2\left(1 + \psi_{k,x_n}\right) = \frac{1-\alpha}{K} log_2\left(1 + \psi_{k,x_n}\right) \quad (7)$$

Next, T_k repeats the operation that T_{k-1} did. Now, considering the last time slot (K-th time slot); T_{K-1} sends the superimposed signal $x_{K-1}^{\oplus} = \sum_{n=1}^{N} \sqrt{a_n P_{T_{K-1}}}\, x_n$ to all the destinations. Also, the destination $T_{K+1,n}$ performs SIC to obtain its desired data x_n. In addition, because the transmit power allocated to the signal x_N is lowest, T_{K-1} performs TAS for $T_{K,N}$. Similar to (5), the channel gain of the $T_{K-1} - T_{K,N}$ link is written as:

$$\gamma_{T_{K-1}^{(t_{K-1})}T_{K,N}^{(r_{K,N})}} = \max_{a=1,\ldots,L}\left(\max_{b=1,\ldots,L}\left(\gamma_{T_{K-1}^{(a)}T_{K,N}^{(b)}}\right)\right) \quad (8)$$

Where:
t_{K-1} and $r_{K,N}$ are the selected transmit and receive antennas at T_{K-1} and $T_{K,N}$, respectively.
For the channel gains of the $T_{K-1} - T_{K,n}$ links $(n \neq N)$; because SC is performed at $T_{K,n}$, we can write:

$$\gamma_{T_{K-1}^{(t_{K-1})}T_{K,n}^{(r_{K,n})}} = \max_{b=1,\ldots,L}\left(\gamma_{T_{K-1}^{(t_{K-1})}T_{K,n}^{(b)}}\right) \quad (9)$$

Where:
$r_{K,n}$ is the selected receive antenna of $T_{K,n}$.
Similar to (6)-(7), the instantaneous SNRs and channel capacity obtained at the destinations can be given, respectively as:

$$\psi_{K,x_n} = \frac{\mu a_n \Delta X_{K-1}^{\text{sum}}\gamma_{T_{K-1}^{(t_{K-1})}T_{K,n}^{(r_{K,n})}}}{(\sum_{i=n+1}^{N} a_i)\mu\Delta X_{k-1}^{\text{sum}}\gamma_{T_{k-1}^{(t_{k-1})}T_k^{(r_k)}}+1}(n < N),\text{and}\psi_{K,x_N} = \mu a_N \Delta X_{K-1}^{\text{sum}}\gamma_{T_{K-1}^{(t_{K-1})}T_{K,N}^{(r_{K,N})}} \quad (10)$$

$$C_{K,x_n} = \frac{(1-\alpha)}{K}\log_2\left(1+\psi_{K,x_n}\right) \quad (11)$$

Due to the DF MHR approach, the e2e instantaneous channel capacity of x_n can be expressed by:

$$C_{\text{e2e},x_n} = \min_{k=1,2,\ldots,K}\left(C_{k,x_n}\right) \quad (12)$$

Finally, the total e2e throughput of the proposed scheme can be formulated as in [21]:

$$\text{TP}_{\text{NOMA}} = \frac{(1-\alpha)}{K}C_{\text{th}}\sum_{n=1}^{N} Pr\left(C_{\text{e2e},x_n} \geq C_{\text{th}}\right) \quad (13)$$

Where:
C_{th} is a pre-determined target rate.

For baseline comparison, this paper also considers the RF-EH aided MHR without using NOMA (named OMA). In orthogonal multiple access (OMA), the e2e throughput of this model can be formulated as:

$$\text{TP}_{\text{OMA}} = \frac{(1-\alpha)}{K}C_{\text{th}}\,Pr\left(C_{\text{e2e}}^{\text{OMA}} \geq C_{\text{th}}\right) \quad (14)$$

Where:

$$C_{\text{e2e}}^{\text{OMA}} = \min_{k=1,2,\ldots,K}\left((1-\alpha)\tau\log_2\left(1+\mu\Delta X_{k-1}^{\text{sum}}\gamma_{T_{k-1}^{(t_{k-1})}T_k^{(r_k)}}\right)\right)$$

With

$$\gamma_{T_{k-1}^{(t_{k-1})}T_k^{(r_k)}} = \max_{a=1,\ldots,L}\left(\max_{b=1,\ldots,L}\left(\gamma_{T_{k-1}^{(a)}T_k^{(b)}}\right)\right)$$

3. PERFORMANCE ANALYSIS

At first, we calculate $Pr\left(C_{\text{e2e},x_n} \geq C_{\text{th}}\right)$ in (13) with $n < N$. Using (7), (10)-(12), we have

$$Pr\left(C_{\text{e2e},x_n} \geq C_{\text{th}}\right) = \prod_{k=1}^{K} Pr\left(C_{k,x_n} \geq C_{\text{th}}\right) = \prod_{k=1}^{K} Pr\left(\frac{\mu a_n \Delta X_{k-1}^{\text{sum}}\gamma_{T_{k-1}^{(t_{k-1})}T_k^{(r_k)}}}{(\sum_{i=n+1}^{N} a_i)\mu\Delta X_{k-1}^{\text{sum}}\gamma_{T_{k-1}^{(t_{k-1})}T_k^{(r_k)}}+1} \geq \theta_{\text{th}}\right), \quad (15)$$

Where:
$\theta_{\text{th}} = 2^{\frac{C_{\text{th}}}{(1-\alpha)\tau}} - 1$. In (15), if $a_n - \theta_{\text{th}}(\sum_{i=n+1}^{N} a_i) \leq 0$, $Pr\left(C_{\text{e2e},x_n} \geq C_{\text{th}}\right) = 0$.

Ortherwise, we rewrite (15) as:

$$Pr\left(C_{\mathrm{e2e},x_n} \geq C_{\mathrm{th}}\right) = \prod_{k=1}^{K} Pr\left(X_{k-1}^{\mathrm{sum}}\gamma_{T_{k-1}^{(t_{k-1})}T_k^{(r_k)}} \geq \rho_{\mathrm{th},n}\right)$$
$$= \prod_{k=1}^{K}\int_0^{+\infty}\left(1 - F_{\gamma_{T_{k-1}^{(t_{k-1})}T_k^{(r_k)}}}\left(\frac{\rho_{\mathrm{th},n}}{z}\right)\right) f_{X_{k-1}^{\mathrm{sum}}}(z)dz \tag{16}$$

Where:
$\rho_{\mathrm{th},n} = \frac{\theta_{\mathrm{th}}}{\left[\left(a_n - \theta_{\mathrm{th}}\left(\sum_{i=n+1}^{N} a_i\right)\right)\mu\Delta\right]}$.

In (16), $F_{\gamma_{T_{k-1}^{(t_{k-1})}T_k^{(r_k)}}}(.)$ is CDF of $\gamma_{T_{k-1}^{(t_{k-1})}T_k^{(r_k)}}$, and from (5) and (9), we obtain:

$$\begin{cases} F_{\gamma_{T_{k-1}^{(t_{k-1})}T_k^{(r_k)}}}(z) = \left[F_{\gamma_{T_{k-1}^{(a)}T_k^{(b)}}}(z)\right]^{L^2} = \left(1 - exp\left(-\lambda_{T_{k-1}T_k}x\right)\right)^{L^2} = 1 + \sum_{v=1}^{L^2}(-1)^v C_{L^2}^v\, exp\left(-v\lambda_{T_{k-1}T_k}x\right), \text{if} k < K \\ F_{\gamma_{T_{K-1}^{(t_{K-1})}T_{K,n}^{(r_{K,n})}}}(z) = \left[F_{\gamma_{T_{K-1}^{(t_{K-1})}T_{K,n}^{(b)}}}(z)\right]^{L} = \left(1 - exp\left(-\lambda_{T_{K-1}T_{K,n}}x\right)\right)^{L} = 1 + \sum_{v=1}^{L}(-1)^v C_L^v\, exp\left(-v\lambda_{T_{K-1}T_{K,n}}x\right) \end{cases} \tag{17}$$

Also in (16), $f_{X_{k-1}^{\mathrm{sum}}}(z)$ is PDF of X_{k-1}^{sum}. Because $X_{k-1}^{\mathrm{sum}} = \sum_{m=1}^{L}\gamma_{\mathrm{BT}_{k-1}^{(m)}}$, using [7, eq. (41)], we have:

$$f_{X_{k-1}^{\mathrm{sum}}}(z) = \frac{\left(\lambda_{\mathrm{BT}_{k-1}}\right)^L}{(L-1)!} z^{L-1}\, exp\left(-\lambda_{\mathrm{BT}_{k-1}}z\right) \tag{18}$$

Substituting (17) and (18) into (16), using [23, eq. (3.471.9)], we obtain:

$$Pr\left(C_{\mathrm{e2e},x_n} \geq C_{\mathrm{th}}\right) = \prod_{k=1}^{K-1}\left[\sum_{v=1}^{L^2}(-1)^{v+1}\frac{2C_{L^2}^v}{(L-1)!}\left(v\lambda_{T_{k-1}T_k}\lambda_{\mathrm{BT}_{k-1}}\rho_{\mathrm{th},n}\right)^{\frac{L}{2}} K_L\left(2\sqrt{v\lambda_{T_{k-1}T_k}\lambda_{\mathrm{BT}_{k-1}}\rho_{\mathrm{th},n}}\right)\right]$$
$$\times\left[\sum_{v=1}^{L}(-1)^{v+1}\frac{2C_L^v}{(L-1)!}\left(v\lambda_{T_{K-1}T_{K,n}}\lambda_{\mathrm{BT}_{K-1}}\rho_{\mathrm{th},n}\right)^{\frac{L}{2}} K_L\left(2\sqrt{v\lambda_{T_{K-1}T_{K,n}}\lambda_{\mathrm{BT}_{K-1}}\rho_{\mathrm{th},n}}\right)\right] \tag{19}$$

Where:
$K_L(.)$ is L-th modified Bessel function of the second kind [23].
With the same derivation manner, as $n = N$, we also obtain:

$$Pr\left(C_{\mathrm{e2e},x_N} \geq C_{\mathrm{th}}\right) = \prod_{k=1}^{K-1}\left[\sum_{v=1}^{L^2}(-1)^{v+1}\frac{2C_{L^2}^v}{(L-1)!}\left(v\lambda_{T_{k-1}T_k}\lambda_{\mathrm{BT}_{k-1}}\rho_{\mathrm{th},N}\right)^{\frac{L}{2}} K_L\left(2\sqrt{v\lambda_{T_{k-1}T_k}\lambda_{\mathrm{BT}_{k-1}}\rho_{\mathrm{th},N}}\right)\right]$$
$$\times\left[\sum_{v=1}^{L^2}(-1)^{v+1}\frac{2C_{L^2}^v}{(L-1)!}\left(v\lambda_{T_{K-1}T_{K,n}}\lambda_{\mathrm{BT}_{K-1}}\rho_{\mathrm{th},N}\right)^{\frac{L}{2}} K_L\left(2\sqrt{v\lambda_{T_{K-1}T_{K,n}}\lambda_{\mathrm{BT}_{K-1}}\rho_{\mathrm{th},N}}\right)\right] \tag{20}$$

Where:
$\rho_{\mathrm{th},N} = \frac{\theta_{\mathrm{th}}}{(a_N\mu\Delta)}$.
Finally, substituting (19)-(20) into (13), we obtain an exact formula of $\mathrm{TP}_{\mathrm{NOMA}}$.

For the OMA scheme, similarly, it is straightforward to obtain that:

$$\mathrm{TP}_{\mathrm{OMA}} = \frac{(1-\alpha)}{K} C_{\mathrm{th}} \prod_{k=1}^{K}\left[\sum_{v=1}^{L^2}(-1)^{v+1}\frac{2C_{L^2}^v}{(L-1)!}\left(v\lambda_{T_{k-1}T_k}\lambda_{\mathrm{BT}_{k-1}}\omega_{\mathrm{th}}\right)^{\frac{L}{2}} K_L\left(2\sqrt{v\lambda_{T_{k-1}T_k}\lambda_{\mathrm{BT}_{k-1}}\omega_{\mathrm{th}}}\right)\right] \tag{21}$$

Where:
$\rho_{\mathrm{th},N} = \frac{\theta_{\mathrm{th}}}{(\mu\Delta)}$.

Next, we propose the power allocation so that all the conditions $a_n - \theta_{\text{th}} \sum_{i=n+1}^{N} a_i > 0$ are satisfied. Indeed, we set $a_n = \xi\theta_{\text{th}} \sum_{i=n+1}^{N} a_i$, where ξ is a constant and $\xi > 1$. Then, with $\sum_{n=1}^{N} a_n = 1$, we have:

$$a_n = \frac{\xi\theta_{\text{th}}}{(1+\xi\theta_{\text{th}})^n} (n < N), \text{and} a_N = \frac{1}{(1+\xi\theta_{\text{th}})^{N-1}}. \quad (22)$$

Finally, we consider TP_{NOMA} and TP_{OMA} at high transmit SNR, i.e., $\Delta \to +\infty$. With (22), it is straightforward that $Pr\left(C_{\text{e2e},x_n} \geq C_{\text{th}}\right) \overset{\Delta\to+\infty}{\approx} 1(\forall n)$. Therefore, we can approximate TP_{NOMA} and TP_{OMA} as:

$$\text{TP}_{\text{NOMA}} \overset{\Delta\to+\infty}{\approx} \frac{(1-\alpha)NC_{\text{th}}}{K}, \text{TP}_{\text{OMA}} \overset{\Delta\to+\infty}{\approx} \frac{(1-\alpha)C_{\text{th}}}{K}. \quad (23)$$

The (23) implies that TP_{NOMA} can be higher N times than TP_{OMA}.

4. SIMULATION RESULTS

Section 4 performs Matlab-based Monte-Carlo simulations [24], [25] to validate the derived fomulas of TP_{NOMA} and TP_{OMA}. We place the source (T_0) and the relays (T_k) at positions$(k/K, 0)$, where $k = 0,1,\ldots,K-1$, and all the destinations are located at (1,0). In addition, the B station is fixed at (0.5, 0.5). For the illustration purpose only, the path-loss exponent, the target rate (C_{th}) and the energy conversion efficiency (η) are fixed by $\beta = 3$, $C_{\text{th}} = 0.5$ and $\eta = 0.25$, respectively. In Figure 2 to Figure 7 (all are drawn by Matlab), the simulation results are denoted by Sim, and the theoretical results are denoted by Theory. We can observe that all the simulation results match very well with the theoretical ones.

Figure 2 presents the e2e throughput of the proposed NOMA scheme and the OMA one as a function of the transmit SNR Δ in dB, with different values of N. As we can see, the e2e throughput of the presented schemes increases as Δ increases because the transmit power of all the nodes increases. However, as Δ is high enough, the e2e throughput converges to the maximum value, as proved in (23). Moreover, as Δ is low, the performance of the proposed NOMA scheme is worse than that of the OMA scheme. Also, at low Δ values, the performance of our scheme is better with lower value of N.

Figure 3 shows the e2e throughput of the NOMA and OMA schemes as a function of Δ in dB, with different values of L. Similar to Figure 2, the proposed scheme only outperforms the OMA scheme at medium and high Δ regions. It is shown that the e2e throughput of both the schemes increases when the number of antennas (L) increases. However, at high Δ values, the e2e throughput of NOMA and OMA converges to the approximate values which do not depend on Δ. It is worth noting that the e2e throughput of both the schemes converges more rapidly with higher value of L.

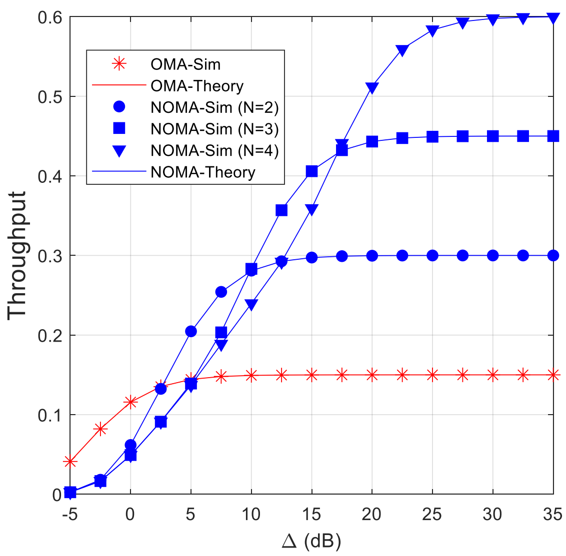

Figure 2. Throughput as a function of Δ (dB) when $K = 3$, $\xi = 2$, $\alpha = 0.1$, and $L = 2$

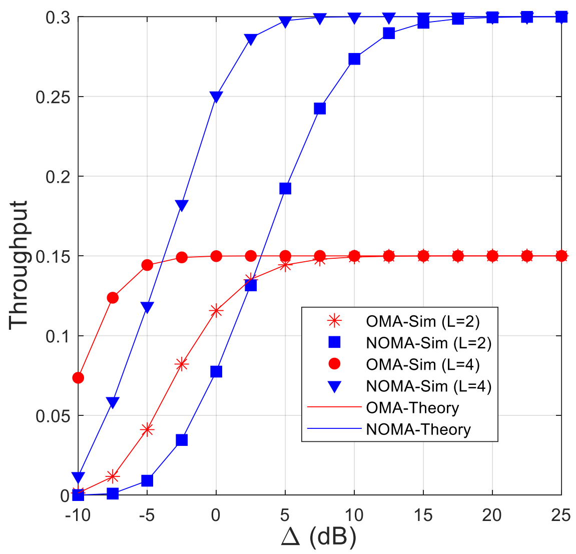

Figure 3. Throughput as a function of Δ (dB) when $K = 3$, $\xi = 3$, $\alpha = 0.1$, and $N = 2$

Figure 4 investigates the impact of the number of hops (K) on the e2e throughput of the NOMA and OMA schemes. As observed, the e2e throughput of all the schemes decreases as K increases. We note that when K increases, the transmission time of each time slot decreases, which also decreases the data rate at each hop. Moreover, we see that with high value of K, the e2e throughput of the NOMA scheme is almost same when N changes. Therefore, our scheme does not perform well as the number of hops is high.

Figure 5 studies the impact of ξ on the throughput performance. From (22), we see that the value of ξ is high, then a_{n-1} is more higher than a_n. Therefore, this is the reason why as $N > 2$, the e2e throughput of the proposed scheme decreases as ξ increases. As ξ is very high, the e2e throughput of our scheme is almost same. It is also seen that with $N = 2$, the performance of the proposed NOMA scheme only changes slightly. More interestingly, the proposed scheme obtains the highest throughput as $N = 3$.

Figure 6 and Figure 7 investigate the impact of α on the e2e throughput of the NOMA and OMA schemes. In Figure 6, we again see that the NOMA scheme is better than the OMA scheme as Δ is high. In both Figure 6 and Figure 7, it is worth noting that there exist optimal values of α, at which the e2e throughput of the NOMA and OMA schemes is highest. However, as α is very high, the e2e throughput of all the presented schemes decreases because the transmission time of the data transmission phase decreases. In Figure 7, the OMA scheme obtains better performance when α is small. Also in Figure 7, the performance of the NOMA scheme is worsest with $N = 4$, and with $N = 3$, the e2e throughput of the NOMA scheme is highest for a wide range of α.

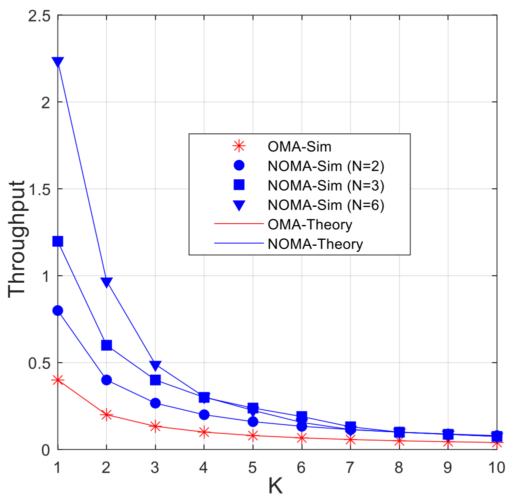

Figure 4. Throughtput as a function of K when $\Delta = 20$ (dB), $\xi = 2$, $\alpha = 0.2$, and $L = 3$

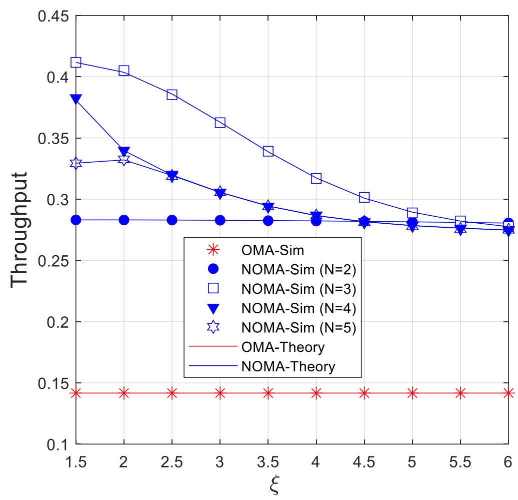

Figure 5. Throughtput as a function of ξ when $\Delta = 10$ (dB), $K = 3$, $\alpha = 0.15$, and $L = 3$

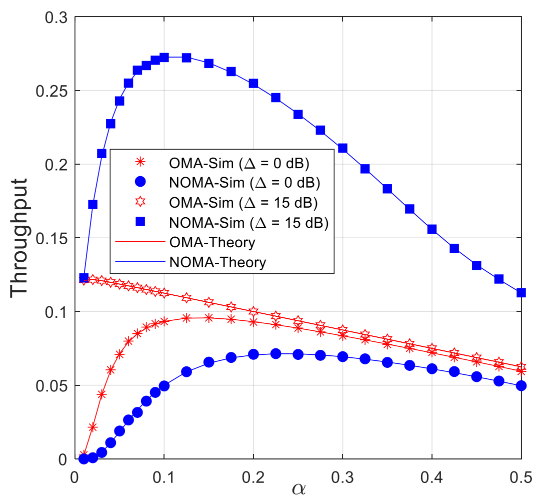

Figure 6. Throughtput as a function of α when $K = 4$, $N = 3$, $\chi = 2$, and $L = 2$

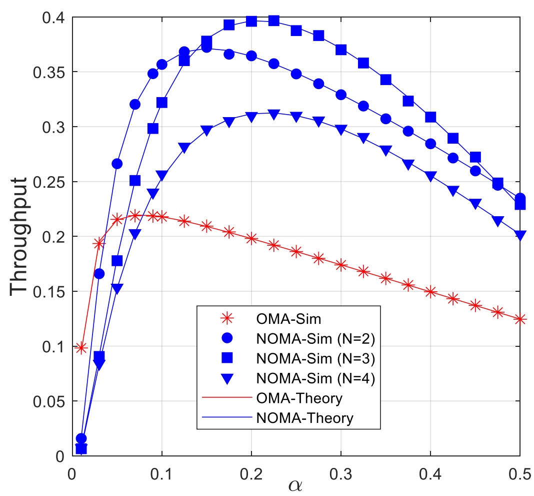

Figure 7. Throughtput as a function of α when $K = 2$, $\Delta = 7.5$ (dB), $\chi = 2$, and $L = 2$

5. CONCLUSION

This paper proposed the wirelessly energy harvesting based multi-hop relaying scheme adopting the TAS/SC and NOMA techniques which can enhance the end-to-end throughput N times, as compared with the corresponding OMA scheme. The results also presented that the proposed scheme does not perform well at low transmit SNR regime and high number of hops. Moreover, the e2e throughput of the proposed scheme can be enhanced significantly by optimally designing the system parameters such as the number of hops (K), fraction of time allocated for the energy harvesting phase (α) and the power allocation coefficient (ξ).

REFERENCES

[1] M. O. Hasna and M. S. Alouini, “Outage Probability of Multihop Transmission over Nakagami Fading Channels,” *IEEE Communications Letters*, vol. 7, no. 5, pp. 216-218, 2003, doi: 10.1109/LCOMM.2003.812178.

[2] C. Conne and I. M. Kim, “Outage Probability of Multi-hop Amplify-and-Forward Relay Systems,” *IEEE Transactions on Wireless Communications*, vol. 9, no. 3, pp. 1139-1149, 2010, doi: 10.1109/TWC.2010.03.090609.

[3] G. Farhadi and N. C. Beaulieu, “Fixed Relaying Versus Selective Relaying in Multi-hop Diversity Transmission Systems,” *IEEE Transactions on Communications*, vol. 58, no. 3, pp. 956-965, 2010, doi: 10.1109/TCOMM.2010.03.070409.

[4] M. R. Bhatnagar, “Performance Analysis of a Path Selection Scheme in Multi-Hop Decode-and-Forward Protocol,” *IEEE Communications Letters*, vol. 16, no. 12, pp. 1980-1983, 2012, doi: 10.1109/LCOMM.2012.100812.121664.

[5] A. Pandey, S. Yadav, D. -T. Do, and R. Kharel, “Secrecy Performance of Cooperative Cognitive AF Relaying Networks With Direct Links Over Mixed Rayleigh and Double-Rayleigh Fading Channels,” *IEEE Transactions on Vehicular Technology*, vol. 69, no. 12, pp. 15095-15112, 2020, doi: 10.1109/TVT.2020.3034729.

[6] P. M. Nam, T. T. Duy, and P. V. Ca, “Performance of Cluster-based Cognitive Multihop Networks under Joint Impact of Hardware Noises and Non-identical Primary Co-channel Interference,” *TELKOMNIKA (Telecommunication, Computing, Electronics and Control)*, vol. 17, no. 1, pp. 49-59, 2019, doi: 10.12928/telkomnika.v17i1.9543.

[7] F. S. Al-Qahtani, R. M. Radaydeh, S. Hessien, T. Q. Duong, and H. Alnuweiri, “Underlay Cognitive Multihop MIMO Networks With and Without Receive Interference Cancellation,” *IEEE Transactions on Communications*, vol. 65, no. 4, pp. 1477-1493, 2017, doi: 10.1109/TCOMM.2016.2627574.

[8] M. Z. Alam, I. Adhicandra, and A. Jamalipour, “Optimal Best Path Selection Algorithm for Cluster-Based Multi-Hop MIMO Cooperative Transmission for Vehicular Communications,” *IEEE Transactions on Vehicular Technology*, vol. 68, no. 9, pp. 8314-8321, 2019, doi: 10.1109/TVT.2019.2917695.

[9] Z. Ding, Z. Yang, P. Fan, and H. V. Poor, “On the Performance of Non-Orthogonal Multiple Access in 5G Systems with Randomly Deployed Users,” *IEEE Signal Processing Letters*, vol. 21, no. 12, pp. 1501-1505, 2014, doi: 10.1109/LSP.2014.2343971.

[10] Z. Ding, M. Peng, and H. V. Poor, “Cooperative Non-Orthogonal Multiple Access in 5G Systems,” *IEEE Communications Letters*, vol. 19, no. 8, pp. 1462-1465, 2015, doi: 10.1109/LCOMM.2015.2441064.

[11] Z. Ding, H. Dai and H. V. Poor, “Relay Selection for Cooperative NOMA,” *IEEE Wireless Communications Letters*, vol. 5, no. 4, pp. 416-419, 2016, doi: 10.1109/LWC.2016.2574709.

[12] H. T. Madan and P. I. Basarkod, “An Optimized Power Allocation Algorithm for Cognitive Radio NOMA Communication,” *TELKOMNIKA (Telecommunication, Computing, Electronics and Control)*, vol. 19, no. 4, 2021, doi: 10.12928/telkomnika.v19i4.20366.

[13] T. T. Phu, T. H. Dang, T. D. Tran, and M. Voznak, “Security-Reliability Analysis of NOMA–Based Multi-Hop Relay Networks In Presence Of an Active Eavesdropper With Imperfect Eavesdropping CSI,” *Advances in Electrical and Electronic Engineering*, vol. 15, no. 4, pp. 591-597, 2017, doi: 10.15598/aeee.v15i4.2386.

[14] P. N. Son and H. Y. Kong, “Cooperative Communication With Energy Harvesting Relays Under Physical Layer Security,” *IET Communications*, vol. 9, no. 17, pp. 2131–2139, 2015, doi: 10.1049/iet-com.2015.0186.

[15] K. H. -Van and T. D. -Dac, “Relay Selection for Security Improvement in Cognitive Radio Networks with Energy Harvesting,” *Wireless Communications and Mobile Computing*, vol. 2021, pp. 1–16, 2021, doi: 10.1155/2021/9921782.

[16] N. P. Le, “Throughput Analysis of Power-Beacon-Assisted Energy Harvesting Wireless Systems Over Non-Identical Nakagami-m Fading Channels,” *IEEE Communications Letters*, vol. 22, no. 4, pp. 840-843, 2018, doi: 10.1109/LCOMM.2017.2756053.

[17] T. N. Nguyen, P. T. Tin, P. T. Tran, T. H. Q. Minh, and M. Voznak, “Power-Splitting Protocol in Power Beacon-assisted Energy Harvesting Full-Duplex Relaying Networks: Performance Analysis,” *2018 11th IFIP Wireless and Mobile Networking Conference (WMNC)*, 2018, pp. 1-7, doi: 10.23919/WMNC.2018.8480900.

[18] X. Wu, L. Tang, and J. Yang, “Outage Performance of Power Beacon-Assisted Cooperative Hybrid Decode-Amplify-Forward Relaying Wireless Communications,” *2020 IEEE/CIC International Conference on Communications in China (ICCC)*, 2020, pp. 1330-1335, doi: 10.1109/ICCC49849.2020.9238898.

[19] C. Xu, M. Zheng, W. Liang, H. Yu, and Y. C. Liang, “Outage Performance of Underlay Multihop Cognitive Relay Networks With Energy Harvesting,” *IEEE Communications Letters*, vol. 20, no. 6, pp. 1148-1151, 2016, doi: 10.1109/LCOMM.2016.2547985.

[20] C. Xu, M. Zheng, W. Liang, H. Yu, and Y. C. Liang, “End-to-end Throughput Maximization for Underlay Multi-hop Cognitive Radio Networks with RF Energy Harvesting,” *IEEE Transactions on Wireless Communications*, vol. 16, no. 6, pp. 3561-3572, 2017, doi: 10.1109/TWC.2017.2684125.

[21] P. T. Tin, P. M. Nam, T. T. Duy, P. T. Tran, T. N. Kieu, and M. Voznak, “Throughput Analysis of Power Beacon-Aided Multi-hop Relaying Networks Employing Non-Orthogonal Multiple Access With Hardware Impairments,” in *Proc. of the 5th AETA 2018 - Recent Advances in Electrical Engineering and Related Sciences: Theory and Application*, 2018, pp. 371-381, doi: 10.1007/978-3-030-14907-9_36.

[22] V. N. Vo, C. So-In, D. Tran, and H. Tran, “Optimal System Performance in Multihop Energy Harvesting WSNs Using Cooperative NOMA and Friendly Jammers,” *IEEE Access*, vol. 7, pp. 125494–125510, 2019, doi: 10.1109/ACCESS.2019.2939385.

[23] I. S. Gradshteyn and I. M. Ryzhik, *Table of Integrals, Series, and Products*, 6th ed. San Diego, CA (USA): Academic Press, 2000. [Online]. Available: http://fisica.ciens.ucv.ve/~svincenz/TISPISGIMR.pdf

[24] D. -B. Ha, S. Q. Nguyen, and H. T. Nguyen, “Cooperative Cognitive Non-Orthogonal Multiple Access under Unreliable Backhaul Connections,” *Mobile Networks and Applications*, vol. 24, pp. 596-617, 2019, doi: 10.1007/s11036-018-1161-5.

[25] D. -H. Ha, T. T. Duy, P. N. Son, T. Le- Tien, and M. Voznak, "Security-Reliability Trade-Off Analysis for Rateless Codes-Based Relaying Protocols Using NOMA, Cooperative Jamming and Partial Relay Selection," in IEEE Access, vol. 9, pp. 131087-131108, 2021, doi: 10.1109/ACCESS.2021.3114343.

BIOGRAPHIES OF AUTHORS

Pham Minh Nam received the B.E degree in 1999 and M.E degree in 2010 from Ho Chi Minh City University of Technology (HCMUT). He became a lecturer at Electronics Engineering Faculty, Industrial University of Ho Chi Minh City (IUH) in 2010. He is participating in Ph. D program at Ho Chi Minh City University of Technology and Education (HCMUTE) in next spring. His major research interests are energy harvesting, multi-hops in communication, performance of cognitive radio and physical layer security. He can be contacted at email: phamminhnam@iuh.edu.vn.

Thanh-Long Nguyen graduated in information technology in 2003 from University of Science, Ho Chi Minh City, Vietnam. In 2011, he received Master degree in Computer Science from Hue University, Thua Thien-Hue Province, Vietnam. He has taught in the information technology at Ho Chi Minh City University of Food Industry (former Junior College of Food Industry) since 1999. In 2021, he graduated and received the Ph. D diploma at VSB-Technical University of Ostrava in the Czech Republic. His research interests include Applied Informatics, Knowledge Discovery, Data Mining, Information and Communications Technology. He can be contacted at email: longnt@hufi.edu.vn.

Ha Duy Hung received B.S. and M.S. degrees in Electronics and Telecommunications Engineering from Institute of Post and Telecommunication, Viet Nam; University of transport and communications, Ha Noi, Vietnam in 2007 and 2014. In 2017, he joined Faculty of Electrical and Electronics Engineering of Ton Duc Thang University, Vietnam as a lecturer. In 2021, he is degrees Ph. D in communication technology at VSB Technical University of Ostrava, Czech Republic. His major interests are cooperative communications, and physical-layer security. He can be contacted at email: haduyhung@tdtu.edu.vn.

Tran Trung Duy received the B.E. degree from HoChiMinh City University of Technology, Vietnam in 2007. In 2013, he received the Ph.D degree from University of Ulsan, South Korea. From 2013, he joined Posts and Telecommunications Institute of Technology (PTIT), Ho Chi Minh city campus. His major research interests are cognitive radio, physical-layer security, hardware impairments and Fountain codes. He can be contacted at email: trantrungduy@ptithcm.edu.vn.

Nguyen Thanh Binh received the PhD degree in 1995. He is currently Vice-Dean of Department of Electrical Engineering, Posts and Telecommunications Institute of Technology (PTIT), Ho Chi Minh city campus. His major research interests are image processing, signal processing and communication. He can be contacted at email: binhnt@ptithcm.edu.vn.

Nguyen Luong Nhat was born in 1969**.** In 1995, he received the PhD degree in telecommunications from Moscow Technical University of Communications and Informatics, Russia. He is currently Dean of Department of Electrical Engineering, Posts and Telecommunications Institute of Technology (PTIT), Ho Chi Minh city campus. His major research interests are signal processing for wireless communication. He can be contacted at email: nhatnl@ptithcm.edu.vn.